Asian Journal of Basic Science & Research
Volume 6, Issue 2, Pages 50-63, April-June 2024

Impact of Incorporating Silver Nanoparticles (AgNPs) into Collagen-PU-PEG Hydrogels for Superior Antibacterial Efficacy in Severe Wounds

Juan J. Mendoza-Villafaña[1], Valeria E. Fuantos-González[1], María I. León-Campos[1], Denis A. Cabrera Munguía[1], Lucía F. Cano-Salazar[1], Tirso E. Flores-Guía[1], Rebeca Betancourt Galindo[2] & Jesús A. Claudio-Rizo[1*]

*[1]Facultad de Ciencias Químicas, Universidad Autónoma de Coahuila, Ing. J. Cárdenas Valdez S/N, República, 25280 Saltillo, Coahuila, México. [2]Centro de Investigación en Química Aplicada, Enrique Reyna H. 140, San José de los Cerritos, 25294 Saltillo, Coahuila, México. Corresponding Author (Jesús A. Claudio-Rizo) Email: jclaudio@uadec.edu.mx**

DOI: http://doi.org/10.38177/AJBSR.2024.6203

Copyright © 2024 Juan J. Mendoza-Villafaña et al. This is an open-access article distributed under the terms of the Creative Commons Attribution License, which permits unrestricted use, distribution, and reproduction in any medium, provided the original author and source are credited.

Article Received: 14 February 2024 *Article Accepted: 25 April 2024* *Article Published: 30 April 2024*

ABSTRACT

Wound healing is a complex process often hindered by microbial infections, particularly in severe wounds like diabetic ulcers and burns. Collagen-based hydrogels offer potential solutions but lack mechanical support and antibacterial properties. This study explores the incorporation of silver nanoparticles (AgNPs) into Collagen-Polyethylene Glycol (PEG) hydrogels crosslinked with polyurethane (PU) for enhanced wound healing. The hydrogels, labeled CPEG-Ag, revealed a dense fibrillar structure resulting from an interconnected matrix; they exhibited superabsorbent swelling capacity (up to 2100%), which increased with AgNPs content from 0 to 5 wt.%, with no significant effects on the crosslinking (%). FTIR spectroscopy demonstrated the formation of a semi-interpenetrating polymeric network, chemically linked by urea bonds and physically by hydrogen bond interactions. *In vitro* cell viability studies showed non-cytotoxic effects on monocytes and fibroblast cells, with the former displaying the best metabolic activity after 48 hours of evaluation, while the latter exhibited high proliferation during the first 24 hours, indicating the safe use of CPEG-Ag hydrogels. The effective antibacterial activity against Gram-negative bacteria, *E. coli*, was also studied, demonstrating that even low contents of AgNPs are sufficient for significant bacterial inhibition. These results highlight the potential of CPEG-Ag hydrogels for wound dressings, especially in complex wounds, and pave the way for future tissue regeneration applications.

Keywords: Collagen-PEG-polyurethane; CPEG-Ag hydrogels; Silver nanoparticles (AgNPs); Semi-IPN; Antibacterial capacity; Wound dressings; Wound healing; Biomedicine; Scaffolds; Tissue regeneration.

1. Introduction

Tissue regeneration is a multifaceted biological process that requires a highly coordinated immune response, cell proliferation, cellular differentiation, and tissue morphogenesis [1]. However, in the case of severe wounds such as diabetic ulcers or those derived from burns, unfavorable microbial environments during the repair process can delay healing or generate very low-quality healing due to microbial infections or impaired angiogenesis [2]. Therefore, the development of materials capable of accelerating and maintaining the complex series of events for appropriate tissue repair is crucial, and further research is necessary [3].

Collagen-based hydrogels have demonstrated promising potential in wound healing and tissue engineering applications due to their attractive fibrillar structure, biodegradability, high biocompatibility, and ability to promote key cellular functions such as adhesion, proliferation, and cell differentiation [4]. However, one drawback of collagen-based hydrogels is their lack of mechanical support, leading to high degradation rates and having a weak resistance against bacterial growth. Chemical crosslinkers, such as polyurethane (PU), have been satisfactorily employed to enhance both the mechanical properties and degradation control of collagen [5-7]. This combination leads to the formation of an interpenetrating polymer network (IPN) system [8]. These hydrogels can be combined with various polymers with functionalities that allow for the improvement and modulation of properties such as biocompatibility, drug release capability, enhanced antibacterial capacity, and facilitation of tissue regeneration. One of these polymers is polyethylene glycol (PEG), a biocompatible synthetic material approved by the FDA for use in biomedical applications [9]. PEG is an inert polymer with high hydrophilicity, and its incorporation into

collagen-based hydrogels help improve the mechanical stability of the materials, providing better structural integrity and making them suitable for scaffold uses [10,11]. Furthermore, the incorporation of PEG improved the performance in the healing of chronic wounds. In general, the incorporation of PEG into the collagen-PU system will offer the development of a semi-IPN platform with tailored properties to meet many requirements involved in tissue regeneration [12].

On the other hand, as mentioned above, one of the most significant issues during the healing process in hard burns, chronic wounds, and diabetic ulcers is the appearance of uncontrollable infections, leading to low-quality healing and, in some critical cases, death [2]. This phenomenon is related to the resistance of many bacteria to traditional antibiotics. Therefore, developing new materials for addressing this healthcare problem must include biomaterials capable of loading antibiotics or efficient alternatives. One of these attractive alternatives is the use of silver nanoparticles (AgNPs), known for their great microbial activity. Nowadays, they have regained relevance by being incorporated into different polymeric matrices for several biomedical applications [13,14].

Massod et al. [15] reported that incorporating AgNPs into the Chitosan-PEG system generates formulations capable of accelerating the healing of chronic diabetic wounds. These tests were evaluated in rabbits, and the presence of silver nanoparticles improved the antimicrobial and antioxidant properties compared to hydrogels without AgNPs. The collagen-PEG combination to generate hydrogels with engineering tissue utility was reported by Timothy D. Sargeant et al. [10] the authors highlighted the importance of collagen in cellular adhesion and facilitating the enzymatic degradation process, while the presence of PEG helped bind proteins in cytocompatibility. Collagen-PEG hydrogels showed tunable mechanical and swelling properties. These characteristics and biological properties made these materials capable of being used as injectable tissue scaffolds to treat tissue regeneration necessities. Alarcon et al. [16] fabricated collagen-coated AgNPs incorporated into collagen-based hydrogels and evaluated the antibacterial properties *in vitro* against *S. aureus, S. epidermidis, E. coli, and P. aeruginosa*, and the inflammatory effects *in vivo* in mice. Their results demonstrated the safety and efficacy of these collagen-AgNPs hydrogels for tissue engineering applications, indicating their potential clinical uses.

Considering the above information, the aim of the work presented here is to expand the use of AgNPs, avoiding cytotoxicity [17] by incorporating them into semi-interpenetrated networks (semi-IPN) formed by Collagen-PU-PEG hydrogels. The synthesized hydrogels were labeled as CPEG-Ag, which were proved effective against E. coli bacteria in *in vitro* assays. Furthermore, we examined the kinetic polymerization of the hydrogels and evaluated their chemical composition, swelling, and crosslinking. The viability properties for monocytes and fibroblast cells are also included. All these characteristics highlight the possibility of using these materials in *in vivo* tests for future tissue regeneration applications, specifically in complex wounds such as burns and diabetic ulcers.

1.1. Study Objectives

The following are the main objectives of this study. (i) Synthesize and evaluate the impact of AgNPs incorporated into hydrogels composed of Collagen-PU-PEG. (ii) Evaluate the physicochemical characteristics such as swelling capacity, crosslinking index, and morphology of the CPEG-Ag Hydrogels synthesized. (iii) Evaluate the chemical composition and the kinetic polymerization of the CPEG-Ag Hydrogels. (iv) Demonstrate the correct metabolic

activity of important cells in the wound healing process: monocytes and fibroblasts. (v) Demonstrate the superior antibacterial properties of CPEG-Ag hydrogels against *E. coli* bacteria.

2. Materials and Methods

2.1. Materials

Collagen type I (Col) (α1=230 000 g mol^{-1} and α2=110 000 g mol^{-1}) was extracted through decellularization/ enzymatic procedures from porcine tendons obtained from pig legs at the local market. Polyethylene glycol (M_n=400), silver nanoparticles (<100 nm particle size), hexamethylene diisocyanate (HDI), glycerol ethoxylate (GE), 3-(4,5-Dimethyl-2-thiazolyl)-2,5-diphenyl-2H-tetrazolium bromide (MTT), 2,2-dihydroxy-1,3-indanedione (ninhydrin), sodium hydroxide, sodium chloride, calcium chloride and other salts were acquired from Merck-Aldrich. The *Escherichia coli* (*E. coli*) bacterial strain (EC11303), eosin-methylene blue (EMB) agar, Dulbecco's Modified Eagle Medium (DMEM), 2-propanol, and other common solvents were acquired from Merck-Aldrich, as well. All reagents were used as received without prior purification processes.

Table 1. Formulations for CPEG-Ag hydrogels

Hydrogel	Collagen (mg)	[a]PU (mg)*	PEG (mg)*	AgNPs (□g)*
CPEG-Ag0	6	1.2	1.2	0
CPEG-Ag0.25	6	1.2	1.2	15
CPEG-Ag0.5	6	1.2	1.2	30
CPEG-Ag1	6	1.2	1.2	60
CPEG-Ag3	6	1.2	1.2	180
CPEG-Ag5	6	1.2	1.2	300

*Amounts of polyurethane (PU) crosslinker (20 wt.%), PEG (20 wt.%) and AgNPs (0.25-5 wt.%), were adjusted based on the collagen concentration (6 mg mL^{-1}). [a]PU was prepared in lab using HDI + GE according to previous reports [18,19].

2.2. Synthesis of CPEG-Ag hydrogels

For triplicated, in a 24-well culture plate kept at 4 °C, 1 mL of collagen type I (6 mg mL^{-1}) was mixed with constant amounts of polyurethane crosslinker (20 wt.%) and polyethylene glycol (20 wt.%). Then, the desired volume of AgNPs from a starting solution (0.5 m/v %) was added to each well containing the previous mix. Finally, a pH=7.4 of the mix was adjusted using 250 µL of a phosphate buffer solution (PBS-10X). All components were vigorously mixed and incubated at 37 °C for 4 h. The formulations of hydrogels are summarized in Table 1.

2.3. Physicochemical characterization of hydrogels

FTIR-ATR analysis was performed on a Perkin-Elmer Frontier spectrophotometer, using a resolution of 4 cm^{-1} and 32 scans for the acquisitions. Optical microscopy (OM) was performed on a VELAB VE-403 inverted microscope.

Kinetic polymerization was monitored by a turbidimetry assay using a UV-Vis ThermoScientific MultiSkan Sky spectrophotometer through absorbance measurements. The swelling capacity of each formed hydrogel was evaluated by triplicate. The initial weight W_i was recorded, and after drying for 72 h, their mass was measured again W_f. The swelling capacity was calculated using Equation 1:

$$\text{Swelling capacity } (\%) = \frac{W_i - W_f}{W_f} * 100 \quad (1)$$

The crosslinking index (%) of each hydrogel was also determined in triplicated using the ninhydrin test. This procedure involves one hydrogel, 1 mL of ninhydrin solution (1 wt.%, pH= 5 in citrate buffer), and 3 mL of deionized water. The reaction was performed using a ThermoScientific dry bath set at 90 °C for 2 hours [20]. Absorbance readings at 560 nm were taken using a ThermoScientific MultiSkan Sky spectrophotometer. Equation 2 was employed to calculate the crosslinking percentage, where A_{sample} corresponds to the average absorbance of hydrogel samples, while $A_{control}$, corresponds to the absorbance of collagen without PU crosslinker.

$$\text{Crosslinking index } (\%) = \left(1 - \frac{A_{sample}}{A_{Control}}\right) * 100 \quad (2)$$

2.4. Cell culture, viability, and antibacterial analysis

The cell viability of fibroblasts and human monocytes growing in contact with hydrogel samples was evaluated using the MTT assay. A total of 100 µL of each cell suspension (30 000 cells mL^{-1}) in DMEM culture medium was placed together with 100 µL of leachates from each hydrogel formulation. Simultaneously, 100 µL of PBS-1X sterile solution was used as a control. All experiments were carried out in triplicated, and the evaluation was conducted after 24 and 48 h of incubation at 37 °C. The MTT reagent (1 wt.%) was added to each well, and formazan crystals were formed after 3 hours of incubation. Then, solubilization of crystals in isopropyl alcohol was performed before recording absorbances at 560 nm. Cell viability was evaluated by comparing absorbances values using Equation 3. Here, $A_{control}$ (100% of viability) corresponds to wells with PBS-1X, instead hydrogels leachates.

$$\text{Cell viability } (\%) = \frac{A_{sample}}{A_{Control}} * 100 \quad (3)$$

The bacterial inhibition properties of each formulated hydrogel against *Escherichia coli* were assessed using sterile Petri dishes containing EMB agar. The bacteria were seeded and incubated for 48 h at 35 °C in the presence of the hydrogels. For comparison, a gentamicin solution (200 ppm) was impregned on filter paper and used as reference control. The inhibition capacity was determined by measuring the diameter of the halo formed, representing the absence of bacterial growth. The inhibition capacity against *E. Coli* bacteria was calculated as defined in equation 4.

$$\text{Inhibition capacity of } E.Coli\ (\%) = \frac{Diameter\ of\ halo\ of\ \text{sample}}{Diameter\ of\ halo\ of\ \text{control}} * 100 \quad (4)$$

2.5. Statistical analysis

The means and standard deviations were considered for the data set, and experiments were done by triplicate. The mean of each experimental condition was compared by One-way Analysis of Variance (ANOVA), and the statistical significance was established by applying a Tukey test with a confidence limit of 95% (*p<0.05).

3. Results and discussion

The CPEG-Ag hydrogels, formulated with varying AgNPs content, exhibited manageable handling and a homogeneous color appearance. In the absence of AgNPs, the hydrogels appeared white, whereas with increasing AgNPs content, a light to dark gray coloration was observed. The hydrogels took on a cylindrical shape acquired from the mold in which they were cast. An illustration of the general preparation of these CPEG-Ag hydrogels is provided in Figure 1. The polyurethane crosslinker promoted the assembly and fibril arrangement of collagen, while the incorporation of PEG aided in stabilizing the AgNPs due to the abundant polar groups on its structure [15,21]. Moreover, the combination of these polymers (collagen-PU-PEG) facilitated the formation of a semi-interpenetrated polymer network (semi-IPN) system.

During the formation of CPEG-Ag hydrogels, the stabilized PEG-AgNPs blend in Collagen-PU system directly impacts in the gelation step during the hydrogel formation process. Figure 2 shows the kinetics of the polymerization of CPEG-Ag hydrogels, which involves spectrophotometric measurements of hydrogel turbidity that correlates with polymerization or gelation process. All CPEG-Ag hydrogel samples exhibited turbidimetry curves with sigmoidal behavior. However, depending on the concentration of AgNPs in the formulated hydrogels, a delay in the semi-interpenetrating network formation was observed. The coordination of PEG with the AgNPs and the interactions with collagen and the crosslinker (PU) seems to affect the fibrillogenesis process of collagen, altering the time required to construct the final polymeric matrix (biomatrix) structure; this effect occurs to a greater extent with the increase in the content of AgNPs. Subsequently, the acceleration in the formation of the semi-IPN structures is visualized by a remarkable increase in the absorbance values. Finally, a plateau in the graphs is observed, with no significant variations in absorbance values, indicating the semi-IPNs were fully formed.

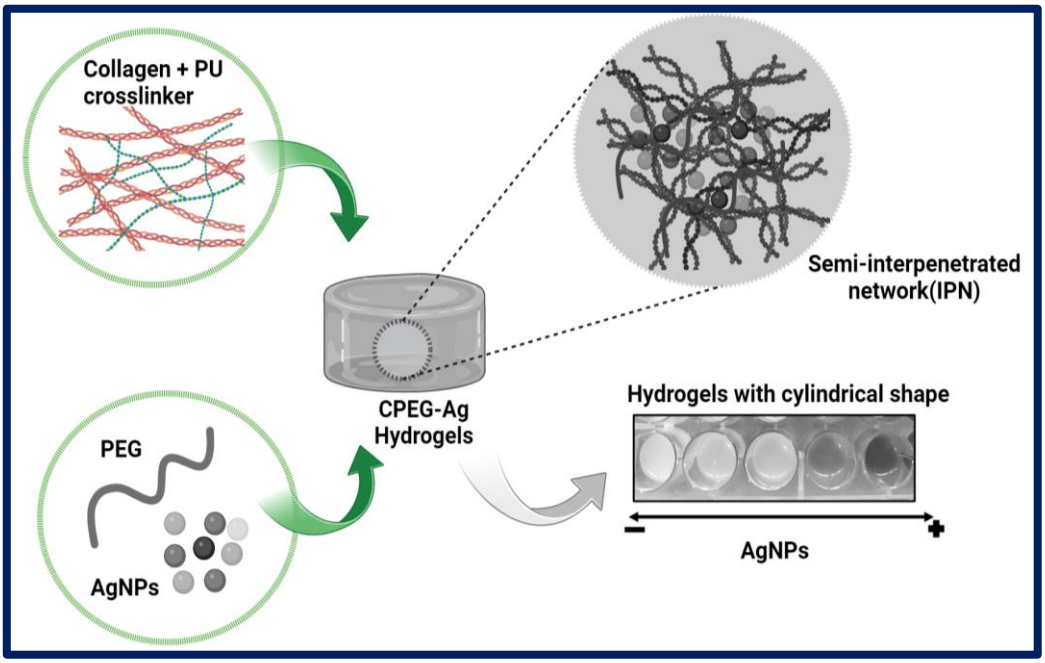

Figure 1. Scheme of the AgNPs incorporation into Collagen-PU-PEG system to form the CPEG-Ag hydrogels. The process involves the formation of semi-interpenetrated networks (semi-IPN), through chemical and physical bonds formation.

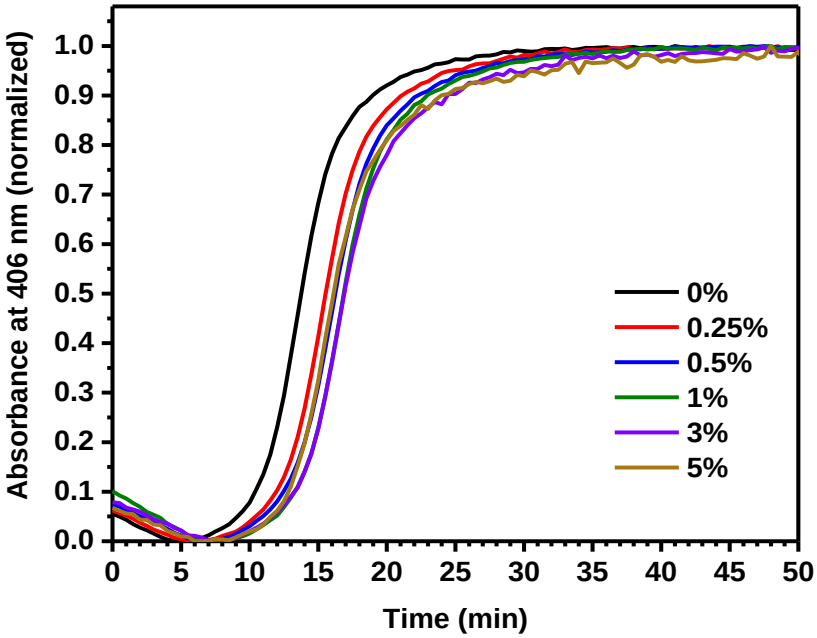

Figure 2. Polymerization kinetic curves for CPEG-Ag hydrogels with variable AgNPs content (0.25-5 wt.%), due to change in turbidity at 406 nm

The chemical structure of the CPEG-Ag hydrogels was analyzed using infrared spectroscopy, and the FTIR spectra are shown in Figure 3. All spectra exhibit a similar pattern across the wavenumber window. In the range of 3550-3200 cm^{-1}, two overlapping bands associated with the stretching vibrations of N-H and O-H bonds from collagen, as well as by the presence of PEG, which is rich in hydroxyl groups, are observed. The absorption bands located at 2920 and 2855 cm^{-1} correspond to the absorption of C-H bonds from aliphatic groups in both structures. At lower wavenumber values, between 1290 cm^{-1} - 1034 cm^{-1}, absorption bands corresponding to the stretching vibrations of C-O and C-O-C are observed.

In the zoomed zone of Figure 3, between 1850-1200 cm^{-1}, the characteristic absorption bands for collagen can be distinguished: amide I at 1654 cm^{-1}, amide II at 1548 cm^{-1}, and a weaker band associated with amide III at 1240 cm^{-1}. Alongside these amide absorptions, the presence of the urea group in the spectra provides strong evidence of the chemical crosslinking in the system formed by collagen-polyurethane, with the associated band appearing around 1740 cm^{-1} corresponding to the C=O group. Since the amount of PEG has no variation among all CPEG-Ag hydrogels, any expected difference in the chemical composition throughout the entire FTIR spectra would depend on the AgNPs content. However, no significant differences were observed. Nevertheless, this type of hydrogel is characterized by forming a semi-interpenetrated network related to both chemical crosslinking (urea formation) and physical crosslinking (hydrogen bonding interactions between polar groups). Taking this in consideration, the stronger intensity of urea group with the increase of AgNPs could be associated with a favored chemical crosslinking, which could have repercussions on the swelling capacity and crosslinking percentages of materials. The increase in the content of silver nanoparticles seems to decrease the intensity of the bands of C-O-C bonds (1100-1000 cm^{-1}), abundant in the semi-IPN system, which indicates that silver tends to occlude in regions with these types of bonds.

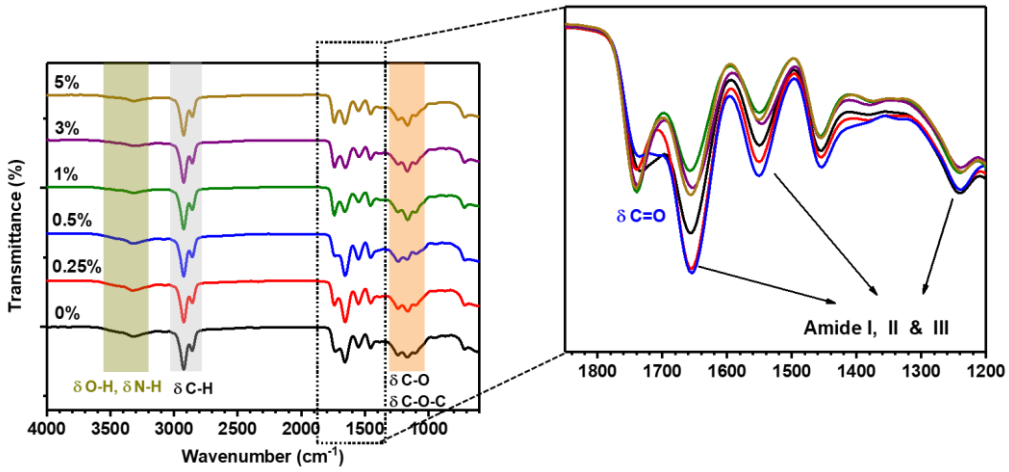

Figure 3. FTIR spectra for CPEG-Ag hydrogels with variable AgNPs content (0.25-5 wt.%)

The design and optimization of a hydrogel with applicability in tissue engineering depends, to some extent, on its swelling capacity, a parameter related to the ability to retain water. This is particularly important as it ensures a suitable environment during regeneration and aids in favoring inflammatory processes. Figure 4a, shows the maximum swelling capacity of the CPEG-Ag hydrogels formulated with different contents of AgNPs and in the absence of them, CPEG-Ag0 hydrogel. In all cases, super-swelling behavior was observed, reaching values above 2100%, with the highest values observed with an increase in AgNPs content in the formulation. Specifically, the CPEG-Ag5 reached a swelling capacity of 2757 ± 102%, which is statistically significant when compared to all other hydrogels. In general, swelling capacities above 1% in the AgNPs content showed statistical significance over the lower AgNPs contents (0-0.5%). These differences could be related to the interaction between the semi-interpenetrated polymeric network formed and the silver nanoparticles. This interaction may occur through electrostatic attraction altering the structure of the hydrogel matrix, where an increase in AgNPs content correlates with a higher water absorption capacity. Pinzaru et al. [21] reported that in the presence of chitosan, the AgNPs interact with the functional groups of polymeric network (-NH_2, -OH). In this case, a similar behavior is expected, not only for the interaction with free NH_2 groups in the collagen but also for the many free hydroxyl groups from PEG, thus the free volume of the biomatrix increase, improving the swelling capacity of hydrogels.

On the other hand, the crosslinking index of the semi-IPN structures, shown in Figure 4b as crosslinking (%), was determined indirectly by the ninhydrin assay, which involves the reaction with free primary amino groups along the collagen structure, resulting in a blue-purple product (Ruhemann's purple). The ratio between absorbance measurements (at 560 nm) of collagen without crosslinker and CPEG-Ag hydrogels allowed to obtain the percentage of crosslinking. Unlike what was observed in the swelling capacity behavior, no significant effects on the crosslinking (%) with respect to the increase in AgNPs were observed, indicating that silver nanoparticles are occluded in the collagen fibrillar matrix, preserving the semi-interpenetrated polymeric network, chemically linked by urea bonds and physically by hydrogen bond interactions, as mentioned earlier. However, from Figure 4b, it is noted that lower AgNPs concentration lightly improves the crosslinking values with 84.6 ± 2% and 83.4 ± 2.5%, corresponding to CPEG-Ag0.5 and CPEG-Ag1 hydrogels, respectively. This is probably due to more crosslinking sites through chemically bonded for these two AgNPs content, as indicated by the stronger C=O band from urea

groups observed by FTIR. Moreover, it is important to highlight that all formulated hydrogels in this work showed a crosslinking index above 76%, which is important for hydrogel state polymeric matrices intended for high efficiency wound dressings. Both swelling capacity and crosslinking degree have influence on the moisture control in wounds, absorption, and removal of exudates, as well as on permeability properties, thereby influenced in the exchange and transport of cell nutrients, allowing the stimulation of cellular metabolism. In addition, they are associated with the surface characteristics and morphology of hydrogels.

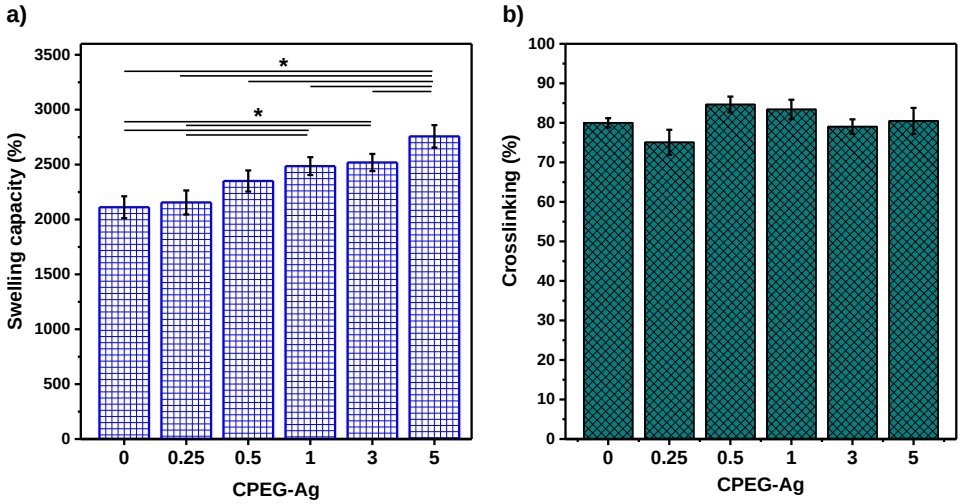

Figure 4. a) Swelling capacity (%) and b) Crosslinking index (%) of and CPEG-Ag hydrogels

The morphology of CPEG-Ag hydrogels was analyzed, and the microstructure of their surface is shown in Figure 5. A dense fibrillar structure resulting from an interconnected matrix is present in all samples, which is common in crosslinked collagen hydrogels [20]. By increasing the content of AgNPs, clustered regions within the interconnected fibrillar matrix and spherical particles corresponding to the presence of silver nanoparticles are observed. As the content of the AgNPs increases, the morphology becomes more discontinuous and saturated with more regions where the nanoparticles are concentrated.

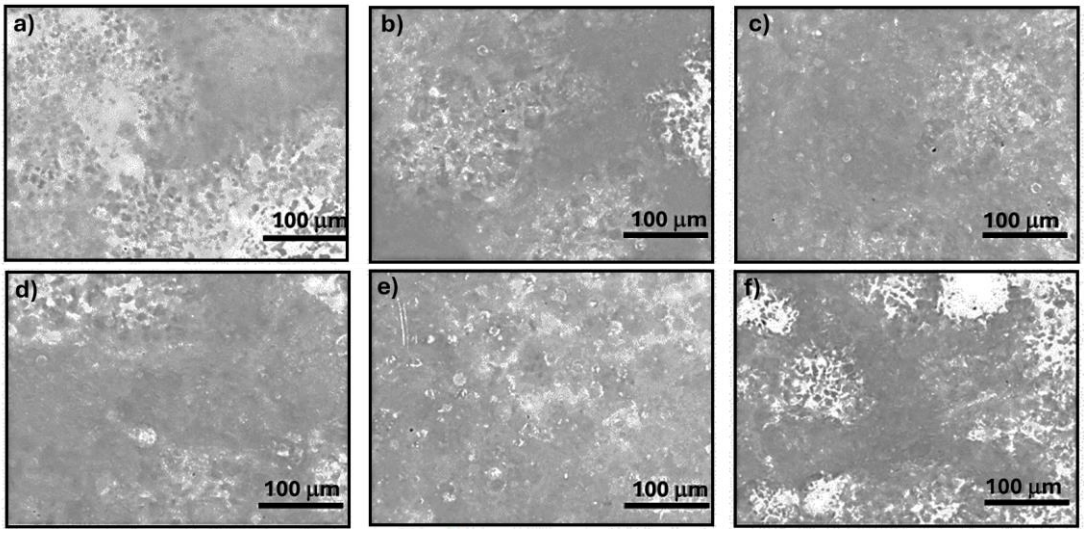

Figure 5. Stereoscopic micrographs of CPEG-Ag samples with different Ag contents: a) 0 wt.%, b) 0.25 wt.%, c) 0.5 wt.%, d) 1 wt.%, d) 3 wt.% and e) 5 wt.%

This phenomenon is related to the electrostatic repulsion interactions between the semi-IPN of Collagen-PU-PEG and the AgNPs. It is important to preserve the organized collagen fibrils within the hydrogel structure, as they play an important role in the biocompatibility properties of the hydrogels, conforming to the irregular shape of complex wounds such as burns and diabetic ulcers. Moreover, this property will ensure cell activity and wound contractions, facilitating the tissue regeneration process. As mentioned, physicochemical properties such as swelling, crosslinking, along morphology are key factors influencing cell viability within hydrogel matrices. Having optimal swelling ensures a supportive microenvironment for cell survival, while an adequate crosslinking density maintains mechanical stability and allows for correct nutrient exchange. On the other hand, morphology, depending on both factors mentioned, must resemble the extracellular matrix, facilitating cell infiltration and adhesion. Therefore, the optimization of these parameters is crucial for effectively managing complex wounds like burns and diabetic ulcers, creating a supportive environment for tissue regeneration, moisture management, and overall wound healing [3,4].

Figures 6a and 6b show the cell viability results of monocytes and fibroblast cell cultures in contact with the biodegradation products (leachates) of CPEG-Ag hydrogels. Monocytes are cells that assist in modulating the inflammatory response, favoring tissue regeneration; in the first 24 hours of evaluation, the results reveal a slow stimulation of the metabolic activity but indicate that any AgNPs content in the hydrogel formulations did not lead to cytotoxic effects on monocytes cell with values above 60% of cell viability. However, the metabolic activity of this cell culture significantly favored cell growth after 48 hours of incubation (above 120% of cell viability), indicating a better adaptability of monocytes over time. Moreover, higher concentrations of silver nanoparticles (3 and 5 wt.%) presented the best viability results, and in all cases the presence of AgNPs showed significant differences in metabolic activity against that sample without AgNPs.

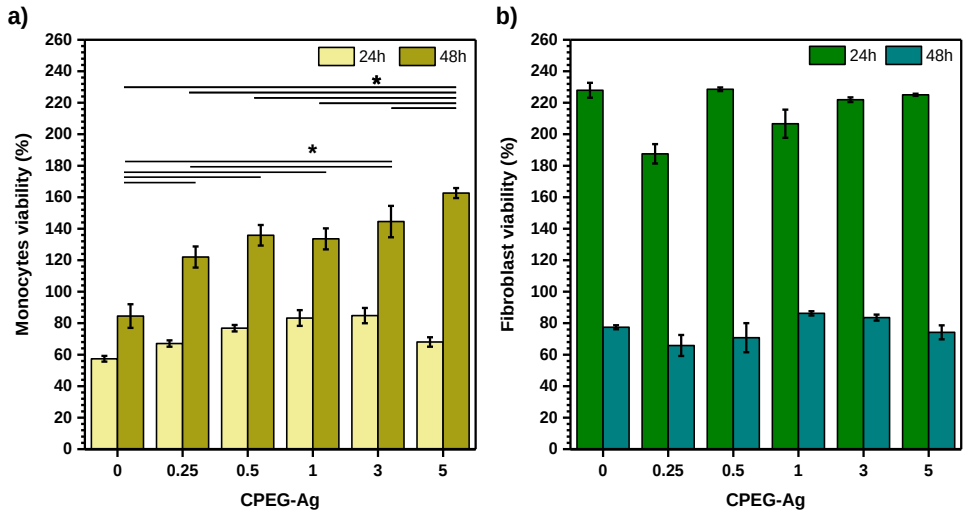

Figure 6. Cell viability (%) by MTT assay for human a) monocytes and b) fibroblasts. Cell cultures were in contact with CPEG-Ag hydrogels during 24 and 48 hours at 37 °C

On the other hand, in the case of fibroblasts cell viability, the chemical composition of the hydrogels clearly did not lead to cytotoxic effects for these cells; on the contrary, it showed cell viability percentages exceeding 180% after 24 hours of incubation. Conversely, during the 48-hours of evaluation, a decrease in metabolic activity of fibroblasts was observed; nonetheless, non-cytotoxic effects were presented. These results, guaranty the

preservation of the metabolic activity of both, monocytes, and fibroblasts, ensuring the safe use of CPEG-Ag hydrogels in applications involving the contact of these materials with these important cells involved in the wound healing process.

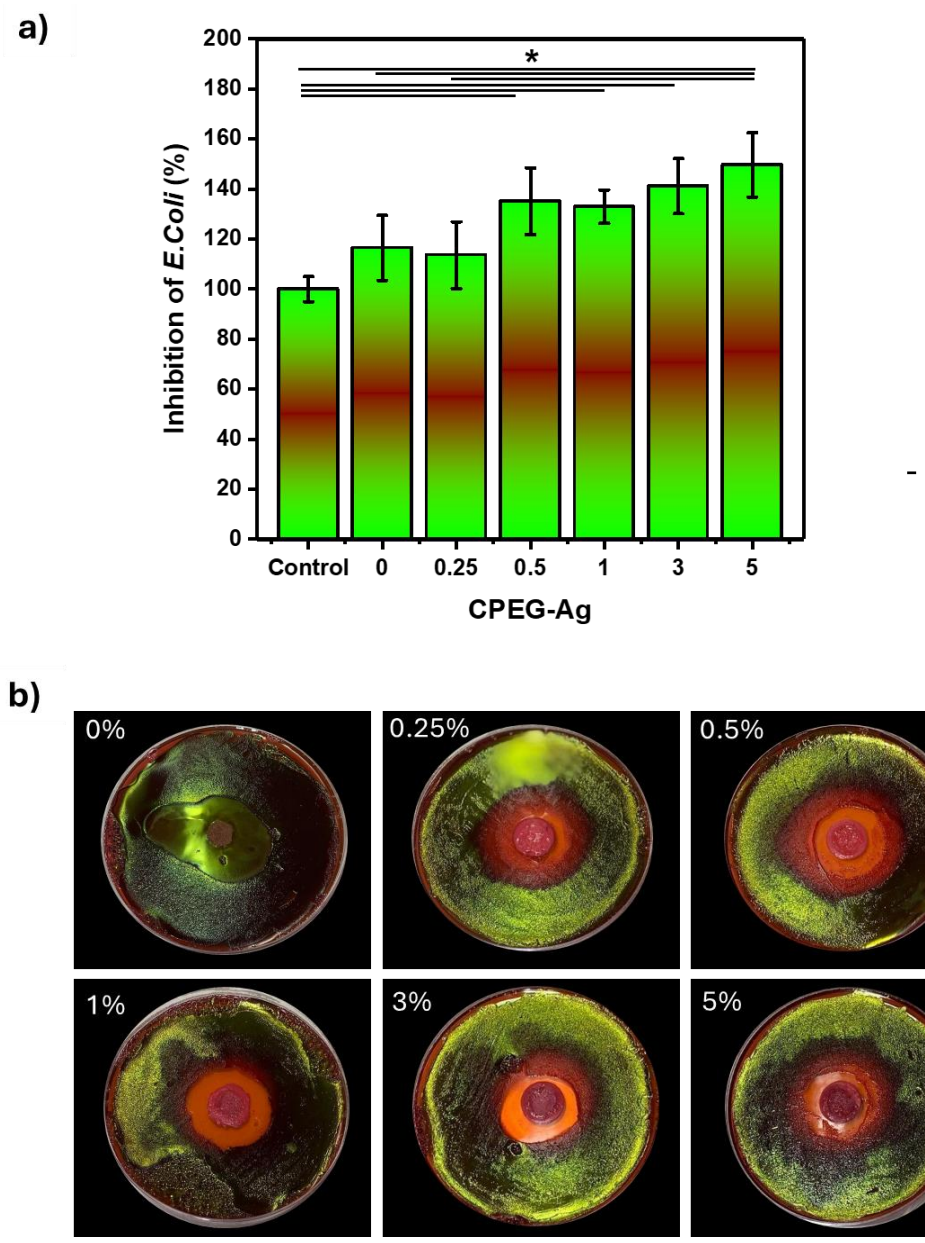

Figure 7. a) Inhibition capacity (%) of CPEG-Ag hydrogels against *Escherichia coli* and b) antibiograms with the inhibition halo where bacteria growth was avoided by the presence of hydrogels

On the other hand, as mentioned earlier, antibiotic-resistant microorganisms are increasing nowadays, making the treatment of infectious wounds, especially severe ones, a challenging task for tissue repair. Antimicrobial activity was assessed in triplicate for each hydrogel formulation containing AgNPs. For this purpose, the inhibition capacity of CPEG-Ag hydrogels against *Escherichia coli* was determined and is shown in Figure 7a. It can be observed that all hydrogels exhibited the capacity to inhibit the *E. coli* growth, with inhibition percentages ranging from 113 ± 13% to 149 ± 12%. Noticeably, the degree of inhibition at all AgNPs concentrations surpassed that of the control, showing statistical significance for those higher than 0.5 %wt., indicating promising potential for this biomatrices

even with a low content of AgNPs incorporation. Measurements of the diameter of the inhibition halo formed (antibiograms), which represent the absence of bacteria growth by the presence of hydrogels, are shown in Figure 7b. The improvement in the inhibition capacity of CPEG-Ag hydrogels is related to the presence of AgNPs, and the increase of their concentration in the biomatrices results in higher antimicrobial activity. The proposal mechanisms of the strong activity of AgNPs against bacteria are varied, but these include the adsorption of AgNPs on bacterial surface, which destabilize the membrane, disrupts electron transport chain, reduces ATP and causes cell death. Other mechanisms include endocytosis through which AgNPs enter bacteria, release silver ions internally, and damage them. In addition, intracellular Ag^{+} ions function as cofactors, inducing oxidative stress by generating ROS (hydroxyl radicals and hydrogen peroxide), damaging bacterial components and potentially leading to cell death [13]. The significance of the inhibition capacity shown by CPEG-Ag hydrogels against bacteria *E. coli* is underscored by the tendency of microorganisms to develop resistance to conventional antibiotics such as gentamicin. The study conducted by Alarcon et al. [16] demonstrated that hydrogels containing AgNPs not only displayed remarkable antibacterial properties against Gram (-) and Gram (+) bacteria but also retained the biocompatibility properties for primary human skin fibroblasts and keratinocytes, while the levels of inflammation markers were reduced. The biocompatibility of CPEG-Ag hydrogels was demonstrated here with the cell viability (%) results by MTT assay for monocytes and fibroblasts cells, as mentioned above. Therefore, the analysis of AgNPs incorporated into CPEG-Ag hydrogels highlighted the safety and efficacy of the hydrogels, making them promising biomatrices for potential application as wound dressings, especially in hard and infected wounds. The results also suggest that a high concentration of AgNPs in the hydrogel may not be necessary for achieving substantial bacterial inhibition, as was demonstrated by CPEG-Ag0.5 hydrogel sample.

4. Conclusions

This study focused on investigating the effects of incorporating AgNPs into Collagen-PEG hydrogels to form semi-interpenetrated networks, utilizing polyurethane as crosslinker. The resulting CPEG-Ag hydrogels, with varying in AgNPs content, exhibited manageable handling and homogeneous appearance. Polyurethane crosslinker facilitated collagen assembly, while PEG stabilized AgNPs. Kinetic polymerization studies revealed delayed network formation with increased AgNPs content, indicating altered fibrillogenesis. FTIR analysis confirmed the formation of a semi-interpenetrated network, with AgNPs influencing the intensity of urea groups. The swelling capacity of hydrogels increased with AgNPs content and showed superabsorbent behavior, while crosslinking was influenced minimally. These physicochemical characteristics, along with a porous morphology, allowed for obtaining cell viability of monocytes and fibroblast while exhibiting high antimicrobial activity against *E. coli* bacteria. These findings highlight the potential for using these materials in future *in vivo* tests for tissue regeneration applications, particularly in treating complex wounds such as burns and diabetic ulcers.

5. Future Suggestions

The study presented in this investigation demonstrated the potential use of the CPEG-Ag hydrogels for tissue regeneration applications. Nonetheless, complementary studies are necessary to fully exploit the potential of these materials. Some of these suggestions are as follows: (i) Investigate the mechanical properties of CPEG-Ag

hydrogels through rheometry under dynamic conditions mimicking physiological movements for their practical application in clinical settings. (ii) Evaluate the biodegradability of CPEG-Ag hydrogels over time under various hydrolytic and enzymatic conditions to ensure tissue regeneration while minimizing inflammatory reactions. (iii) Evaluate the superior antibacterial properties of CPEG-Ag hydrogels against other microorganisms responsible for wound infections, such as *S. Aureus*. (iv) Investigate the capacity of CPEG-Ag hydrogels as drug delivery system for therapeutic agents. (v) Design *in vitro* test to evaluate the efficacy of CPEG-Ag hydrogels in a wound closure assay.

Declarations

Source of Funding

Consejo Nacional de Humanidades, Ciencias y Tecnologías (CONACyT) supported this study with the grant FORDECYT-PRONACES/6660/2020.

Competing Interests Statement

The authors declare that they have no conflict of interest.

Consent for Publication

The authors declare that they consented to the publication of this study.

Authors' Contributions

All the authors took part in literature review, research, and manuscript writing equally.

Availability of data and material

Supplementary information is available from the authors upon reasonable request.

Acknowledgements

The authors acknowledge to Jesús Alfonso Mercado for providing technical support in FTIR analysis.

References

[1] Gurtner, G.C., Werner, S., Barrandon, Y., & Longaker, M.T. (2008). Wound Repair and Regeneration. Nat., 15 (7193): 314–321. https://doi.org/10.1038/nature07039.

[2] Patel, S., Srivastava, S., Singh, M.R., & Singh, D. (2019). Mechanistic Insight into Diabetic Wounds: Pathogenesis, Molecular Targets and Treatment Strategies to Pace Wound Healing. Biomed. Pharmacother., 112: 108615. https://doi.org/10.1016/j.biopha.2019.108615.

[3] Su, J., Li, J., Liang, J., Zhang, K., & Li, J. (2021). Hydrogel Preparation Methods and Biomaterials for Wound Dressing. Life, 11(10): 1016. https://doi.org/10.3390%2Flife11101016.

[4] Zhang, Y., Wang, Y., Li, Y., Yang, Y., Jin, M., Lin, X., Zhuang, Z., Guo, K., Zhang, T., & Tan, W. (2023). Application of Collagen-Based Hydrogel in Skin Wound Healing. Gels, 9: 185. https://doi.org/10.3390/gels 9030185.

[5] Caldera-Villalobos, M., León-Campos, M.I., Claudio-Rizo, J.A., Cabrera-Munguía, D.A., Mendoza-Villafaña, J.J., Cano-Salazar, L.F., & Flores-Guía, T.E. (2023). Hydrophilic Polyurethanes: A Brief Review from the Synthesis to Biomedical Applications. Mediterr J Basic Appl Sci., 7(1): 42–57. https://doi.org/10.46382/MJBAS.2023.7105.

[6] Cui, M., Chai, Z., Lu, Y.; Zhu, J., & Chen, J. (2023). Developments of Polyurethane in Biomedical Applications: A Review. Resour Chem Mater., 2(4): 262–276. https://doi.org/10.1016/j.recm.2023.07.004.

[7] Liang, W., Ni, N., Huang, Y., & Lin, C. (2023). An Advanced Review: Polyurethane-Related Dressings for Skin Wound Repair. Polym., 15(21): 4301. https://doi.org/10.3390/polym15214301.

[8] Claudio-Rizo, J.A., Rangel-Argote, M., Muñoz-González, P.U., Castellano, L.E., Delgado, J., Gonzalez-García, G., Mata-Mata, J.L., & Mendoza-Novelo, B. (2016). Improved Properties of Composite Collagen Hydrogels: Protected Oligourethanes and Silica Particles as Modulators. J Mater Chem B., 4: 6497–6509. https://doi.org/10.1039/C6TB01673A.

[9] Chen, S.L., Fu, R.H., Liao, S.F., Liu, S.P., Lin, S.Z., & Wang, Y.C. (2018). A PEG-Based Hydrogel for Effective Wound Care Management. Cell Transplant., 27(2): 275–284. https://doi.org/10.1177/0963689717749032.

[10] Sargeant, T.D., Desai, A.P., Banerjee, S., Agawu, A., & Stopek, J.B. (2012). An in Situ Forming Collagen–PEG Hydrogel for Tissue Regeneration. Acta Biomater., 8(1): 124–132. https://doi.org/10.1016/j.actbio.2011.07.028.

[11] Chen, J.X., Yuan, J., Wu, Y.L., Wang, P., Zhao, P., Lv, G.Z., & Chen, J.H. (2018). Fabrication of Tough Poly(Ethylene Glycol)/Collagen Double Network Hydrogels for Tissue Engineering. J Biomed Mater Res A., 106(1): 192–200. https://doi.org/10.1002/jbm.a.36222.

[12] Rangel-Argote, M., Claudio-Rizo, J.A., Mata-Mata, J.L., & Mendoza-Novelo, B. (2018). Characteristics of Collagen-Rich Extracellular Matrix Hydrogels and Their Functionalization with Poly(Ethylene Glycol) Derivatives for Enhanced Biomedical Applications: A Review. ACS Appl Bio Mater., 1(5): 1215–1228. https://doi.org/10.1021/acsabm.8b00282.

[13] Pangli, H., Vatanpour, S., Hortamani, S., Jalili, R., & Ghahary, A. (2021). Incorporation of Silver Nanoparticles in Hydrogel Matrices for Controlling Wound Infection. J Burn Care Res., 42(4): 785–793. https://doi.org/10.1093/jbcr/iraa205.

[14] Ruiz, M., De, Y.P., Campos, A., Alves, L.A., Agreles, M.A., Galembeck, A., Macário, F., Cavalcanti, I., Banti, C.N., Hadjikakou, S.K., Patricia, Y., André, L., Andressa, M., Agreles, A., Galembeck, A., Macário, I., & Cavalcanti, F. (2023). Advanced Hydrogels Combined with Silver and Gold Nanoparticles against Antimicrobial Resistance. Antibiot., 12(1): 104. https://doi.org/10.3390/antibiotics12010104.

[15] Masood, N., Ahmed, R., Tariq, M., Ahmed, Z., Masoud, M.S., Ali, I., Asghar, R., Andleeb, A., & Hasan, A. (2019). Silver Nanoparticle Impregnated Chitosan-PEG Hydrogel Enhances Wound Healing in Diabetes Induced Rabbits. Int J Pharm., 559: 23–36. https://doi.org/10.1016/j.ijpharm.2019.01.019.

[16] Alarcon, E.I., Udekwu, K.I., Noel, C.W., Gagnon, L.B.P., Taylor, P.K., Vulesevic, B., Simpson, M.J., Gkotzis, S., Islam, M.M., Lee, C.J., Richter-Dahlfors, A., Mah, T.F., Suuronen, E.J., Scaiano, J.C., & Griffith, M. (2015). Safety and Efficacy of Composite Collagen–Silver Nanoparticle Hydrogels as Tissue Engineering Scaffolds. Nanoscale, 7(44): 18789–18798. https://doi.org/10.1039/C5NR03826J.

[17] Sapkota, K., Narayanan, K.B., & Han, S.S. (2017). Environmentally Sustainable Synthesis of Catalytically-Active Silver Nanoparticles and Their Cytotoxic Effect on Human Keratinocytes. J Clust Sci., 28(3): 1605–1616. https://doi.org/10.1007/s10876-017-1169-1.

[18] Mendoza-Villafaña, J.J., Franco-Martínez, M.G., Claudio-Rizo, J.A., Cabrera-Munguía, D.A., Caldera-Villalobos, M., León-Campos, M.I., Flores-Guía, T.E., & Cano-Salazar, L.F. (2023). Zn-Based Metal-Organic Frameworks (MOFs) Incorporated into Collagen-Polysaccharide-Based Composite Hydrogels for Their Use in Wound Healing. Asian J Basic Sci Res., 5(1): 41–54. https://doi.org/10.38177/AJBSR.2023.5106.

[19] Claudio-Rizo, J.A., Mendoza-Novelo, B., Delgado, J., Castellano, L.E., & Mata-Mata, J.L. (2016). A New Method for the Preparation of Biomedical Hydrogels Comprised of Extracellular Matrix and Oligourethanes. Biomed Mater., 11(3): 035016. https://doi.org/10.1088/1748-6041/11/3/035016.

[20] Claudio-Rizo, J.A., Hernandez-Hernandez, N.G., Cano-Salazar, L.F., Flores-Guía, T.E., de la Cruz-Durán, F.N., Cabrera-Munguía, D.A., & Becerra-Rodríguez, J.J. (2021). Novel Semi-Interpenetrated Networks Based on Collagen-Polyurethane-Polysaccharides in Hydrogel State for Biomedical Applications. J Appl Polym Sci., 138(4): 49739. https://doi.org/10.1002/app.49739.

[21] Pinzaru, I., Coricovac, D., Dehelean, C., Moacă, E.A., Mioc, M., Baderca, F., Sizemore, I., Brittle, S., Marti, D., Calina, C.D., Tsatsakis, A.M., & Şoica, C. (2018). Stable PEG-Coated Silver Nanoparticles – A Comprehensive Toxicological Profile. Food Chem Toxicol., 111: 546–556. https://doi.org/10.1016/j.fct.2017.11.051.